ADAPTIVE GFRP ROTOR BLADES AND ADDITIVE MANUFACTURING OF THE MOLDING TOOLS

Lucas Ost[1], Holger Seidlitz[1,2], Felix Kuke[1,2], Manoja Rao Yellur[1], Jonas Krenz[1], Lars Ulke-Winter[1,2]

[1] *Chair of Polymer-based Lightweight Design, Brandenburg University of Technology Cottbus – Senftenberg (BTU), Germany*
[2] *Research devision Polymeric Materials and Composites PYCO, Fraunhofer Institute for Applied Polymer Research IAP, Germany*

Corresponding author:
Holger Seidlitz
Chair of Polymer-based Lightweight Design
Brandenburg University of Technology Cottbus – Senftenberg (BTU)
Konrad-Wachsmann-Allee 17, 03046 Cottbus, Germany
phone: (+49) 355 69 2344
e-mail: fg-leichtbau@b-tu.de

Abstract

Small wind turbines are mostly designed for strong and medium wind regions, which are scaled by manufacturers based on similarity rules. However, the inland region represents a low wind region where the commercially available blades are not profitable. In this work, a rotor blade was designed for these wind conditions and further performance improvement of the turbine was generated by self-adaptive adjustment of the blades to the variable wind loads. This adaptation is achieved by a ply structure that exhibits bending-torsion coupling. The tooling for the production of the GFRP rotor blades was manufactured using a large-format 3D extrusion printer.

Keywords

Fiber reinforced plastic, lightweight design, adaptive, rotor blade, additive manufacturing.

1. Introduction

Environmental protection and compliance with climate targets are becoming increasingly important [4, 14]. The expansion of renewable energies is a necessary, but also cost-intensive step towards achieving these goals. The resulting increase in the price of electricity, in addition to the desire to make their own contribution [4], is a central motivation for many private individuals to supply themselves partly by means of small wind turbines (SWT).

SWT usually reach their rated power only at 12 m/s and are profitable in coastal areas. At a height of 10 m, however, the average wind speed in inland areas is mostly below 5 m/s [9, 12]. The greatest influence on efficiency is exerted by the rotor blades, which to date have primarily been designed for strong- and medium-wind regions. They are scaled in size by the manufacturers according to similarity rules.

Therefore, the blades are usually not designed for the respective installation site. For this reason, they only start up at wind speeds above 3 m/s and thus have a low power output in low and medium wind regions. Furthermore, when the rated power of a SWT is reached, a short-circuit resistance motor brake kicks in to reduce the speed. This means that part of the generated energy is used for braking.

In order for private household SWT to be profitable in inland areas, they must be designed and implemented for low- and medium-wind regions. For this purpose, two novel approaches are combined and implemented:
1) optimized geometry for low and medium wind regions;
2) independent throttling without motor brake by passive adaptation of the angle of attack to the wind load by means of bending-torsion coupling (BTC).

2. Construction and design

Profiles: The profiles for low wind regions were selected and verified using a design and simulation program (QBlade v0.96.3). A preliminary blade geometry was constructed and simulated from the profiles.

CAD: The rotor, pre-designed by means of a calculation program, was then implemented using a computer-aided design (CAD) program (Rhinoceros 6.0). For this purpose, the profiles used were scaled in size and positioned in space according to the design. Surfaces were then stretched between these profiles and connected to the root and winglet. In the next step, the edges and radii of the design were modified for fiber-compatible manufacturing.

3. Design of the layer structure using numerical calculation methods

Approach: The rotational speed and the power are influenced by the angle of attack of the rotor blade.

A passive adjustment of the angle can be attained via the BTC, so that a starting at low wind speeds and large outputs at higher wind speeds can be achieved.

Fiber-reinforced plastic composites exhibit anisotropic, i.e. direction-dependent, properties. For example, the modulus of elasticity of a unidirectional ply is significantly higher in the fiber direction than perpendicular to the fiber direction. This anisotropy leads to a coupling of the deformations in the case of a fiber orientation deviating from the 0° and 90° directions, as well as for asymmetrical ply sequences. For example, with appropriate fiber orientation, a bending moment can cause not only bending deformation but also twisting [5, 7, 8]. Whether there is coupling can be read in the ABD matrix, which summarizes the stiffnesses of the laminate [10]. The challenge is to find a ply structure that both exhibits bending-torsional coupling and withstands the stresses in use. Since an experimental iterative investigation of suitable layups is very costly, finite element method (FEM) models are used instead.

The loads acting on the rotor blade are the centrifugal force due to rotation and the pressure distributions resulting from the wind load. These complex pressure distributions are not known in advance and must therefore be calculated. Computational fluid dynamics (CFD) under Ansys Fluent 3D is used for this purpose.

CFD: The wind turbine has three rotor blades. To reduce the computational effort, only one blade and only one third of the air volume is modeled in the CFD and periodic boundary conditions are applied correspondingly. An extreme load case is assumed, with a wind speed of 20 m/s and a rotational speed of 460 revolutions per minute.

A mesh with tetrahedron elements and prism layers on the rotor blade wall is created. Ansys Fluent 3D 2020 R1 and Ansys CFD-Post are used for the further model construction, the calculation and the evaluation. The two-equation model SST k-ω is chosen as the turbulence model. This model independently activates the k-ω model in the near wall region and the k-ε model in the free stream region [6]. The pressure-based solver is used to calculate the steady state solution.

As a result, the pressure on the rotor blade (Fig. 1) is exported to an Abaqus deck. The shear forces are very small and are neglected.

FEM: The rotor blade, designed as a hollow structure, is built as an FEM model with several components: the glass fiber reinforced plastic (GFRP) facing sheets, a balsa core in the clamping area and an adhesive seam at the trailing edge. The GFRP shells form a closed mesh in the FEM model and are constructed from S4 and occasional S3R linear shell elements. The thick adhesive seam consists of C3D8 elements. The balsa core is meshed using C3D8 and C3D4 linear solid elements. Both components are bonded to the GFRP shell by tie constraints.
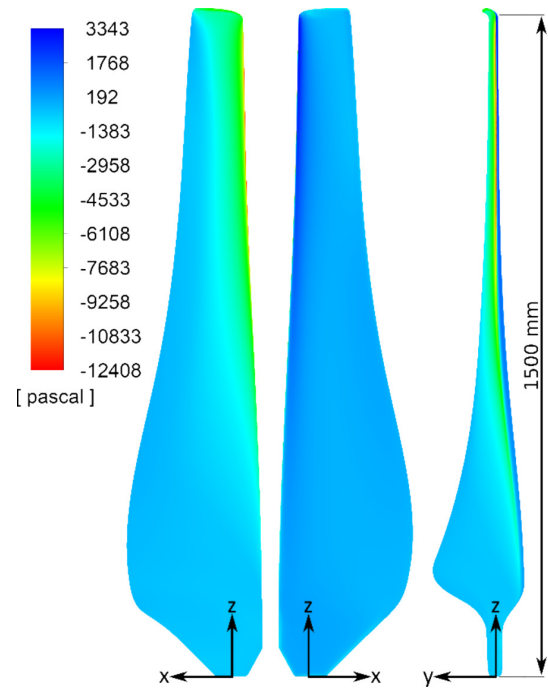

Fig. 1. Static pressure distribution.

The rotor blade is held by four bolts and clamped with two steel plates. The bolts are modeled with C3D8 and C3D6 elements and the plates with S4 elements. A hard contact is defined between the bolts and the steel plates, the GFRP shells and the balsa core (friction coefficient $\mu = 0.05$) as well as between the steel plates and the GFRP shells ($\mu = 0.15$).

The area of the steel plates on which the washers rest in the design are connected with MPCs to one reference node (RN) each per hole and side. The opposite RNs are connected with beam elements. In the first calculation step, a pretension [1] is applied via these to simulate the tightening of the bolts. The compressive forces resulting from the wind load are mapped and applied together with the centrifugal force in the second calculation step. The faces of the steel bolts modeled with solid elements are fixed in both steps. They carry the forces in the plane orthogonal to the wind direction.

Using a Python script, the torsion angle is calculated based on the Abaqus results and used together with the Tsai-Wu failure criterion [11] in the Abaqus CAE for evaluation. The ply structure is iteratively varied until the strength requirements are met, the laminate is optimally loaded, and the highest possible torsion angle is achieved. In addition, the investigated layer structures are evaluated with regard to their manufacturing effort.

The developed blade with asymmetric ply layup achieves significant torsion under wind load compared to a standard $[0/90/\pm 45]$ quasiisotropic layup (Fig. 2). Furthermore, the rotor blade with the standard layout exhibits deformations that reduce efficiency.
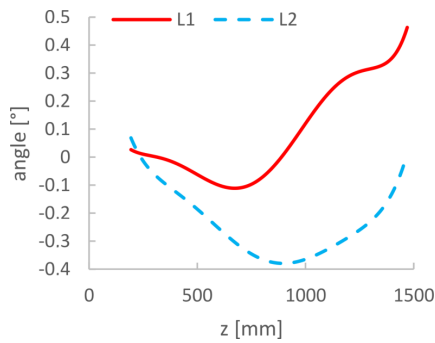
Fig. 2. Torsion angle over rotor blade length (z) for the developed layup (L1) and a standard layup (L2), polynomial regression curves.

4. 3D-printing of manufacturing tools and blade production

3D printing of an FKV-based molding tool: A two-part mold was specially developed for the technical manufacturing realization of the new generation of rotor blades (Fig. 3). For the first time, a direct extrusion system was used that combines both additive and subtractive plastics processing in one system and has also been available at the BTU Institute of Lightweight Design and Value-added Management (ILW) since March 2021.
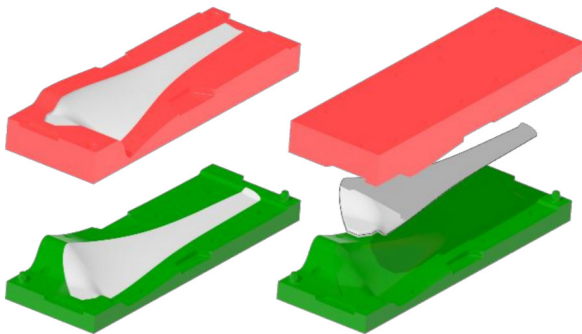

Fig. 3. CAD-model of the two-part blade mold.

Additive manufacturing offers enormous potential for reducing the manufacturing time and cost of the mold for FRP components. A combination of high-volume material application by direct extrusion of thermoplastic pellets and a downstream single-stage subtractive fine finishing process enables the mold to be built quickly and at short notice. This hybrid approach allows economical production of molds for few moldings, mainly due to the high material efficiency as well as the short process times as a result of the high output rates of the extruder during build-up.

Compared to classic toolmaking, a hybrid 3D printing system requires significantly fewer work steps and also considerably reduces component mass by implementing the large-volume tool ($1700 \times 500 \times 350$ mm) as a thin-walled hollow body structure. The printed tool weighs approximately 30 kg. This means that the tool can be handled by two people. In contrast, the mass of

a comparable tool made of aluminum is approx. 500 kg due to its particular design.

The two halves of the mold were fabricated with the Super Discovery hybrid manufacturing cell by its developer, CNC BÁRCENAS BELLÓN S.L. (Fig. 4). The two-stage technology enables direct extrusion of fiber-reinforced plastic granules and the subsequent milling process within one machine. The use of polymers in granule form enables efficient material discharge of up to 25 kg/h. Direct extrusion also favors near-net-shape material application, so that only a single fine finishing operation is required as rework to produce a sufficient surface finish of the mold cavity. Roughing operations are completely eliminated. In this respect, the technology differs from the classic milling process with polyurethane or epoxy resin-based block materials glued to each other, because these would have to be roughened in several milling stages and then finished several times. With suitable parameter selection, efficient, material-saving, near-net-shape 3D printing with a downstream fine finishing process is time-saving, material-efficient and also more cost-effective.

Fig. 4. 3D-printed two-part mold.
Source: CNC BÁRCENAS BELLÓN S.L.

Manufacturing of rotor blades from fiber glass reinforced plastic: The fiber composite rotor blades were manufactured by infusing glass fiber clutches and fabrics with epoxy resin (Fig. 5). Precise positioning for bonding the GFRP shells was performed in the closed mold halves. Following lacquering, the blades were assembled and the rotor was balanced (Fig. 6). Due to the hollow structure of the closed profile and the high specific stiffnesses and strengths of the GFRP [2, 3, 13], the newly developed rotor blades are very light with a weight of 2.5 kg.
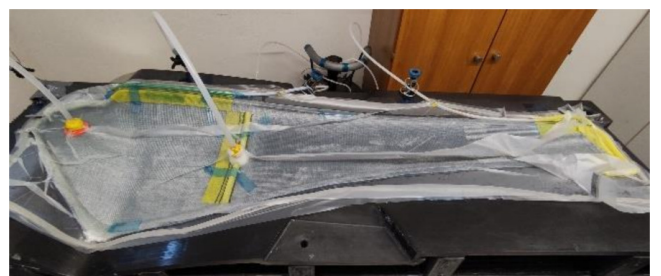

Fig. 5. Setup for resin infusion.

Fig. 6. Setup for balancing the rotor. In the background a hybrid large scale additive manufacturing cell.

Manufacturing of the spinner cap: The spinner cap is the cover of the rotor hub. The master model was made from PLA using fused deposition modeling (FDM) technology. This cost-effective additive manufacturing process enables the rapid implementation of complex geometries with low manpower requirements. This master model was used in the lamination process to produce the forming mold for the spinner cap. At 45 to 60°C, the glass transition temperature of the PLA is very low compared to the operating temperature range of the thermoset resin. This meant that the master model could be removed from the mold manually without the use of large forces.

5. Conclusion

By using powerful calculation and simulation techniques, a fast and substantiated design of an efficient layer structure was achieved and the blade weight was reduced to 2.5 kg. With the most modern manufacturing technologies, the tooling was implemented quickly and cost-effectively. These additively manufactured tools further have low weight as an advantage. The final development step is the testing of the newly developed rotor blades. This is planned in Luckau (Brandenburg, Germany). Here, the energy yield data determined over a year will be compared with the data recorded in 2020 for the classic design.

References

[1] Abaqus 2019 Keywords Guide (2019) *PRE-TENSION SECTION.

[2] Balakrishnan V.S., Hart-Rawung T., Buhl J., Seidlitz H., Bambach M., [*Impact and damage behaviour of FRP-metal hybrid laminates made by the reinforcement of glass fibers on 22MnB5 metal surface*, Composites Science and Technology, 187, 1–15, 2020.

[3] Balakrishnan V.S., Obrosov A., Kuke F., Seidlitz H., Weiß S., *Influence of metal surface preparation on the flexural strength and impact damage behaviour of thermoplastic FRP reinforced metal laminate made by press forming*, Composites Part B: Engineering, 173, 1–10, 2019.

[4] Bouman T., Verschoor M., Albers C.J., Böhm G., Fisher S.D., Poortinga W., Whitmarsh L., Steg L., *When worry about climate change leads to climate action: How values, worry and personal responsibility relate to various climate actions*, Global Environmental Change, 62, 1–11, 2020.

[5] Fedorov V., *Bend-Twist Coupling Effects in Wind Turbine Blades*, Ph.D.-Thesis, Technical University of Denmark, 2012.

[6] Fluent 2020 R1 Theory Guide (2020) 4.4. Standard, BSL, and SST k-ω Models.

[7] Gasch R., Twele J., *Windkraftanlagen Grundlagen, Entwurf, Planung und Betrieb*, 8. edition, Springer Vieweg, Wiesbaden, 2013.

[8] Goeij W.C., Tooren M.J.L., Beukers A., *Implementation of bending-torsion coupling in the design of a wind-turbine rotor-blade*, Applied Energy, 63, 191–207, 1999.

[9] http://www.spiegel.de/wirtschaft/service/strompreis-und-eeg-umlage-oekostrom-umlage-sinkt-2018-leicht-a-1173078.html (03.05.2018).

[10] Mittelstedt C., Becker W., *Strukturmechanik ebener Laminate*, Kapitel 7 Klassische Laminattheorie, Mechanik, Technische Universität Darmstadt, s. 144–169, 2016.

[11] Tsai S.W., Wu E.M., *A General Theory of Strength for Anisotropic Materials*, Journal of Composite Materials, 5, 1, 58–80, 1971.

[12] Windgeschwindigkeiten in der Bundesrepublik Deutschland. Jahresmittel in 10 m über Grund, Bezugszeitraum 1981–2000, Deutscher Wetterdienst, Klima- und Umweltberatung, http://www.wind-of-change.org/files/helix_files/news/160823_Bergedorfer/Windkarte-Deutschland-10m.pdf (23.06.2021).

[13] Yellur M.R., Seidlitz H., Kuke F., Wartig K., Tsombanis N., *A low velocity impact study on press formed thermoplastic honeycomb sandwich panels*, Composite Structures, 225, 1–10, 2019.

[14] 7. United Nations Framework Convention on Climate Change. New York, 9 May 1992.